Plastic distributed feedback laser biosensor

M. Lu, S. S. Choi, U. Irfan, and B. T. Cunningham[a)]
Department of Electrical and Computer Engineering, Micro and Nanotechnology Laboratory, University of Illinois, Urbana, Illinois 61801, USA

(Received 30 July 2008; accepted 28 August 2008; published online 18 September 2008)

A replica-molded plastic-based vertically emitting distributed feedback (DFB) laser has been demonstrated for label-free chemical and biomolecular detection in which the emission wavelength is modulated by changes in bulk and surface-adsorbed material permittivity. A one-dimensional surface grating formed in UV-curable polymer on a flexible plastic substrate is coated with a thin polymer film incorporating organic laser dye. When optically pumped with a ~10 ns pulse at $\lambda = 532$ nm, the DFB laser exhibits stimulated emission in the $\lambda = 585-620$ nm wavelength range with a linewidth as narrow as $\delta\lambda = 0.09$ nm. While exposed to chemical solutions with different refractive indices and adsorbed charged polymer monolayers, the laser sensor demonstrates single mode emission over a tuning range of ~14 nm and the ability to perform kinetic monitoring of surface-adsorbed mass. A protein-protein interaction experiment is used to demonstrate the capability to characterize antibody-antigen affinity binding constants. © *2008 American Institute of Physics*. [DOI: 10.1063/1.2987484]

A wide variety of optical resonator structures have been used for label-free detection of chemical compounds, biomolecules, and cells.[1,2] Several approaches have been commercially developed for application in life science research, environmental monitoring, quality control testing, and diagnostic testing.[3,4] Label-free resonant optical sensors generally detect shifts in resonant wavelength or coupling angle caused by the interaction between the target molecule and the evanescent portion of the resonant modes. The narrow spectral linewidth achieved by using high Q factor ($>10^5$) passive optical resonators enables sensor systems to resolve smaller wavelength shifts associated with the detection of analytes at low concentration, or detection of biomolecules with low molecular weight, such as drug compounds.[5–9] While detection resolution can be substantially improved through the use of high Q factor passive resonators, the sensitivity and dynamic range of the system is generally decreased, although certain examples of passive resonators have achieved high Q factor and high sensitivity simultaneously.[10] In addition, the implementation of high Q factor optical resonators typically requires high precision alignment for evanescent light in/out coupling, providing potential limits to their practical application. Active resonator sensors, such as laser-based optical biosensors,[11–13] have been drawing special interest because they generate their own narrow linewidth stimulated emission, while retaining simple instrumentation and eliminating the requirement for high precision evanescent coupling to waveguides or tapered optical fibers. While our previous work demonstrated distributed feedback (DFB) laser biosensors fabricated on a glass substrate using a sol-gel dielectric grating,[11] practical biosensor applications demand an inexpensive fabrication method that can be performed over large surface areas. A large area, flexible, plastic-based sensor can be easily integrated with standard-format microplates and microarray slides that interface easily with the automated fluid handling and detection instrument infrastructure that are commonly used in life science applications. This work demonstrates a DFB laser biosensor that is fabricated with a plastic-based process on a flexible plastic substrate using a high surface-area nanoreplica molding process.[14] This advance is important to the eventual realization of single-use disposable biosensors made possible by mass-manufacturing of the sensor from continuous sheets of plastic film, in a similar fashion to the manufacturing methods used to produce photonic crystal biosensors.[15]

The DFB cavity demonstrated in this letter is based on a second order Bragg grating that supports a vertically emitting mode by first-order diffraction.[16] A schematic cross-sectional diagram of the designed DFB laser structure is shown in Fig. 1. The low refractive index polymer layer applied to the substrate functions as a cladding layer, upon which a thin film of high refractive index polymer provides vertical light confinement and feedback along the horizontal direction. Doped with laser dye, this high refractive index layer also contributes to the light amplification of the cavity oscillation mode. Altering the refractive index of the media exposed to the DFB laser surface or surface adsorption of biomolecules changes the effective refractive index associated with the resonant mode, and results in modulation of the stimulated emission wavelength. By controlling the guidance layer thickness, the DFB laser is designed to exhibit single

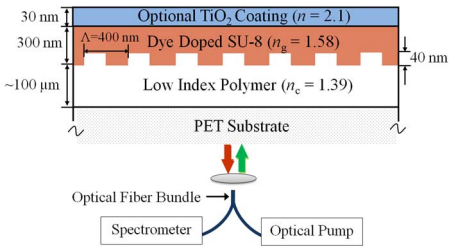

FIG. 1. (Color online) Cross-sectional schematic diagram of the plastic-based DFB laser biosensor. The thickness of the cladding layer is ~100 μm. The laser sensor laser sensor surface was coated with a TiO_2 layer with thickness of 30 nm and refractive index $n = 2.1$.

a)Electronic mail: bcunning@uiuc.edu.

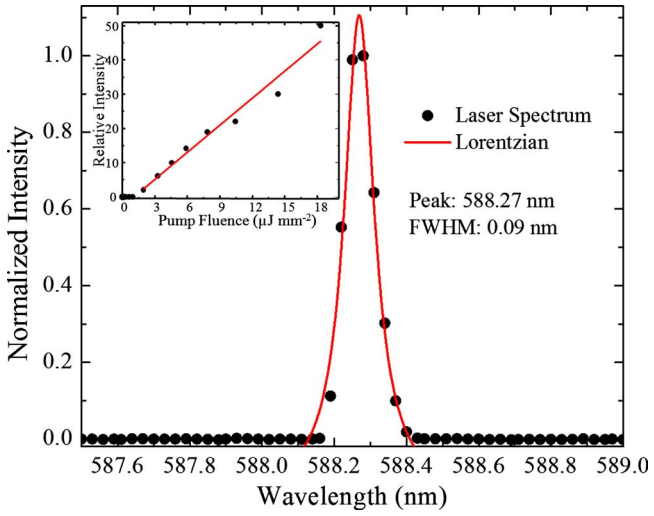

FIG. 2. (Color online) DFB laser emission with the sensor surface exposed to air and pumped at a fluence of 8.5 μJ mm^{-2}. Inset shows the laser threshold curve.

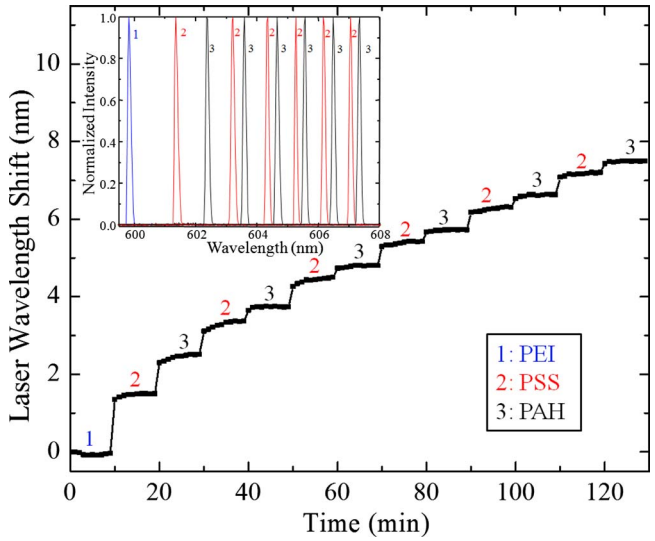

FIG. 3. (Color online) Dynamic detection of alternating layers of positive and negative charged polymer self-limiting monolayers. Inset shows the normalized laser emission spectrum recorded after each deposition.

mode radiation to facilitate determination of the laser wavelength shift.

The one-dimensional grating structure is produced with an ultraviolet (UV) curable polymer on polyethyleneterephthalate (PET) substrate by a nanoreplica molding technique. A liquid UV-curable polymer with $n=1.39$ was squeezed between the PET substrate and a silicon master wafer. The silicon stamp surface was produced by conventional *E*-beam lithography and reactive ion etching. The replicated polymer grating was exposed to O_2 plasma for ~30 s to render a hydrophilic surface. Atomic force microscopy verified that the replicated gratings have a period of $\Lambda=400$ nm and a depth of $d=40$ nm. The active medium was prepared by mixing a 5 mg/ml solution of Rhodamine 590 dye (Exciton) in CH_2Cl_2 with SU-8 (5.0 wt %; Microchem) to a volume percentage of 10%. This mixture was sonicated for improved homogenization and subsequently spin coated onto the previously fabricated grating surface at 5000 rpm for 30 s. The device was soft baked on a 95 °C hotplate for 1 min to remove the solvent, photopolymerized by exposing to UV radiation (365 nm lamp source) with exposure dose of 60 mJ cm^{-2}, and subsequently hard baked on a 95 °C hotplate for 2 min. The gain/waveguide layer has an overall thickness of ~300 nm and refractive index of $n=1.58$ as measured by ellipsometer (VASE, J.A. Woollam). A titanium dioxide (TiO_2) thin film was deposited on top of the DFB laser surface using an electron beam evaporator (Denton Vacuum) to improve biomolecular immobilization and sensor sensitivity.[17]

The DFB laser was optically excited by a frequency doubled, *Q*-switched Nd:YAG (yttrium aluminum garnet) laser ($\lambda=532$ nm, 10 ns pulse width, single pulse mode) through a 600 μm diameter fiber and a focusing lens underneath the sensor surface (Fig. 1). The emission from the DFB laser biosensor was coupled to a spectrometer (HR4000, Ocean Optics) through a detection fiber bundled with the excitation fiber. As illustrated by the inset of Fig. 2, the dependence of the relative laser pulse energy on the pump fluence (measured by a pryoelectric detector) exhibits a clear threshold fluence of 1.09 μJ mm^{-2}. Figure 2 shows the laser spectrum observed with the sensor surface exposed to air while pumped at 8.5 μJ mm^{-2}. The laser emission spectrum was fit to a Lorentzian profile, as shown in Fig. 2, to mathematically determine the center wavelength. Sensitivity to changes in the refractive index of media exposed to the sensor surface was measured by placing a droplet of water ($n=1.333$), acetone ($n=1.359$), isopropyl alcohol ($n=1.377$), and dimethyl sulfoxide ($n=1.479$) upon a single sensor in sequence. Single mode laser emission was measured for each solution, and a bulk refractive index sensitivity of $S_b=\Delta\lambda/\Delta n=99.58$ nm/RIU was measured, with linear behavior over the ~14 nm tuning range (data not shown).

In order to characterize the sensor sensitivity as a function of distance from the sensor surface, stacked alternating positively and negatively charged polyelectrolyte layers were deposited onto the sensor surface, according to the method described in Ref. 15. The polyelectrolytes used in this work were anionic poly(sodium 4-styrenesulfonate) (PSS) ($M_w=60$ kDa), cationic poly(allylamine hydrochloride) (PAH) ($M_w=70$ kDa) and cationic poly(ethylenimine) (PEI) ($M_w=60$ kDa) all dissolved in 0.9*M* NaCl at a concentration of 5 mg/ml. The polyelectrolyte layer coating self-limits to a single monolayer with a refractive index of $n=1.49$ and thickness of ~5 nm. To build up the polymer stack, NaCl buffer was pipetted onto the sensor surface to establish a baseline and then replaced by PEI solution. After 10 min incubation, the PEI solution was removed; and the sensor surface was washed with NaCl buffer. Six PSS-PAH alternating layers were deposited in sequence with a NaCl buffer rinse used after every PSS or PAH incubation. Figure 3 (inset) shows the laser spectra measured at the end of each incubation step. Figure 3 illustrates the temporal progression of the laser wavelength shift for the PEI and six PSS-PAH depositions, while the DFB laser wavelength was recorded at 30 s intervals. It should be noted that the initial PSS-PAH double layers (~10 nm) generate laser wavelength shifts of 2.2 nm with twice the magnitude of the following double layers. Figure 4 shows that a single sensor may be queried many times over a substantial period of time without bleaching of the laser dye, thus enabling study of kinetic profiles of biomolecular adsorption. Figure 4 also illustrates that the

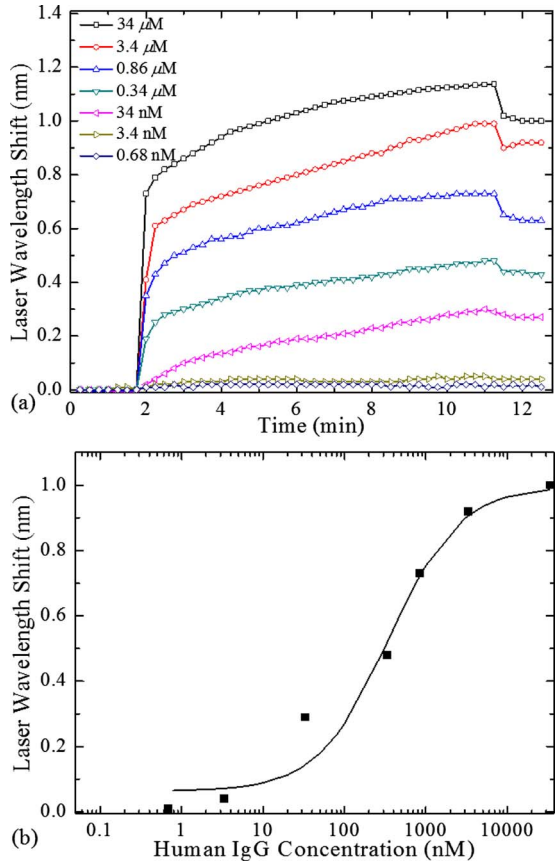

FIG. 4. (Color online) (a) Binding kinetic response of Human IgG exposed at a range of concentrations to a sensor surface prepared with immobilized protein A. (b) Using the laser wavelength shift end point after washing the sensor surface, the dose-response curve for the protein A-human IgG binding interaction with nonlinear curve fitting.

sensor maintains single mode laser output over a wide wavelength dynamic range; and that the sensor wavelength shift response is not saturated after the deposition of a total thickness of ~60 nm material on its surface.

To demonstrate the ability of the sensor to detect biomolecules and to characterize the affinity binding constant of a protein-protein interaction with a simple procedure, protein A was adsorbed to the surface using noncovalent hydrophobic attachment; and subsequently exposed to a human antibody under a range of concentrations. Protein A (Sigma-Aldrich; M_w=40 kDa) was dissolved in 0.01M phosphate buffered saline (PBS; pH=7.4) solution to a concentration of 0.5 mg/ml, pipetted onto sensor surface, and allowed to incubate for 20 min at room temperature. Human IgG (Sigma-Aldrich, M_w=146 kDa) was dissolved in 0.01M PBS solution to seven different concentrations (34, 3.4, 0.86, 0.34 μM and 34, 3.4, and 0.68 nM). Seven different spots on the sensor slide were then rinsed and soaked in PBS buffer to establish an initial baseline emission wavelength. After 3–4 min, the PBS solution was replaced by a human IgG solution and stabilized for 10 min. Then the sensor surface was rinsed with PBS solution to remove any unbound IgG. The detection kinetics for human IgG at different concentrations are shown in Fig. 4(a) with spectra measured every 15 s. Figure 4(b) shows the laser wavelength shift end point as a function of human IgG concentration. The high concentration (>10 μM) human IgG detection approaches saturation due to the limited number of protein A binding sites on the sensor surface. The lowest concentration of human IgG (3.4 nM) resulted in an easily measured laser wavelength shift of $\Delta\lambda \sim 0.05$ nm. As determined by the inflection point of nonlinear curve fitting (Prism, GraphPad Software) the measured dissociation constant is K_d =0.53 μM.

In summary, a plastic-based replica-molded DFB laser biosensor incorporating a UV-curable polymer grating and an organic gain/waveguide layer upon a PET substrate has been demonstrated and characterized. This sensor actively generates its own high intensity narrow bandwidth output and is capable of simultaneously providing high sensitivity, a large dynamic range, and simple excitation/emission coupling without strict alignment requirements. Detection sensitivity to bulk refractive index changes, adsorbed layers of polymers, and adsorbed biomolecules have been demonstrated. Although sensors reported here were produced by hand in small batches, reproducibility as measured by the initial DFB emission wavelength was excellent (within 2 nm over ten devices tested), and would be expected to improve further for devices produced over substantially large surface areas using roll-based fabrication methods.

This work was supported by SRU Biosystems. The authors would like to acknowledge Dr. Edmond Chow of Micro and Nanotehonology Laboratory at University of Illinois at Urbana Champaign.

[1] R. Narayanaswamy and O. S. Wolfbeis, *Optical Sensors: Industrial, Environmental and Diagnostic Applications* (Springer, Berlin, 2004).
[2] A. J. Cunningham, *Introduction to Bioanalytical Sensors* (Wiley, New York, 1998).
[3] B. T. Cunningham, P. Li, S. Schulz, B. Lin, C. Baird, J. Gerstenmaier, C. Genick, F. Wang, E. Fine, and L. Laing, J. Biomol. Screening **9**, 481 (2004).
[4] U. Jonsson, L. Fagerstam, B. Ivarsson, B. Johnsson, R. Karlsson, K. Lundh, S. Lofas, B. Persson, H. Roos, I. Ronnberg, S. Sjolander, E. Stenberg, R. Stahlberg, C. Urbaniczky, H. Ostlin, and M. Malmqvist, BioTechniques **11**, 620 (1991).
[5] I. M. White and X. D. Fan, Opt. Express **16**, 1020 (2008).
[6] A. Yalcin, K. C. Popat, J. C. Aldridge, T. A. Desai, J. Hryniewicz, N. Chbouki, B. E. Little, O. King, V. Van, S. Chu, D. Gill, M. Anthes-Washburn, and M. S. Unlu, IEEE J. Sel. Top. Quantum Electron. **12**, 148 (2006).
[7] C. Y. Chao, W. Fung, and L. J. Guo, IEEE J. Sel. Top. Quantum Electron. **12**, 134 (2006).
[8] N. M. Hanumegowda, C. J. Stica, B. C. Patel, I. White, and X. D. Fan, Appl. Phys. Lett. **87**, 201107 (2005).
[9] F. Vollmer, D. Braun, A. Libchaber, M. Khoshsima, I. Teraoka, and S. Arnold, Appl. Phys. Lett. **80**, 4057 (2002).
[10] I. M. White, H. Oveys, and X. D. Fan, Opt. Lett. **31**, 1319 (2006).
[11] M. Lu, S. Choi, C. J. Wagner, J. G. Eden, and B. T. Cunningham, Appl. Phys. Lett. **92**, 261502 (2008).
[12] W. Fang, D. B. Buchholz, R. C. Bailey, J. T. Hupp, R. P. H. Chang, and H. Cao, Appl. Phys. Lett. **85**, 3666 (2004).
[13] M. Loncar, A. Scherer, and Y. M. Qiu, Appl. Phys. Lett. **82**, 4648 (2003).
[14] J. A. Rogers, M. Meier, A. Dodabalapur, E. J. Laskowski, and M. A. Cappuzzo, Appl. Phys. Lett. **74**, 3257 (1999).
[15] B. Cunningham, B. Lin, J. Qiu, P. Li, J. Pepper, and B. Hugh, Sens. Actuators B **85**, 219 (2002).
[16] R. F. Kazarinov and C. H. Henry, IEEE J. Quantum Electron. **21**, 144 (1985).
[17] I. D. Block, N. Ganesh, M. Lu, and B. T. Cunningham, IEEE Sens. J. **8**, 274 (2008).